Title
Enhanced Thermochemical Heat Capacity of Liquids: Molecular to Macroscale Modeling

Journal
Nanoscale and Microscale Thermophysical Engineering, 23(3)

ISSN
1556-7265

Authors
Yu, Peiyuan
Jain, Anubhav
Prasher, Ravi S

Publication Date
2019-07-03

DOI
10.1080/15567265.2019.1600622

Peer reviewed

Enhanced Thermochemical Heat Capacity of Liquids: Molecular to Macroscale Modeling

Peiyuan Yu,[a] *Anubhav Jain,*[*,a] *and Ravi S. Prasher*[*,a,b]

[a]Energy Storage and Distributed Resources Division, Lawrence Berkeley National Laboratory, Berkeley, California 94720, United States

[b]Department of Mechanical Engineering, University of California, Berkeley, California 94720, United States

* E-mail: ajain@lbl.gov; rsprasher@lbl.gov

Abstract

Thermal fluids have many applications in the storage and transfer of thermal energy, playing a key role in heating, cooling, refrigeration, and power generation. However, the specific heat capacity of conventional thermal fluids, which is directly linked to energy density, has remained relatively low. To tackle this challenge, we explore a thermochemical energy storage mechanism that can greatly enhance the heat capacity of base fluids (by up to threefold based on simulation) by creating a solution with reactive species that can absorb and release additional thermal energy. Based on the classical theory of equilibrium thermodynamics, we developed a macroscale theoretical model that connects fundamental properties of the underlying reaction to the thermophysical properties of the liquids. This framework allows us to employ state-of-the-art molecular scale computational tools such as density functional theory calculations to identify and refine the most suitable molecular systems for subsequent experimental studies. Our approach opens up a new avenue for developing next-generation heat transfer fluids that may break traditional barriers to achieve high specific heat and energy storage capacity.

Introduction

Thermal energy storage plays a broad and important role in transforming our energy economy [1, 2]. With over 90% of the world's primary energy generation consumed or wasted thermally, technologies for the efficient storage and transfer of heat have numerous applications and huge impact on reducing energy-related emissions and improving energy efficiency [3]. As the typical thermal energy storage medium and carrier, thermal fluids (or heat transfer fluids) are critical in heating, ventilation, and air conditioning (HVAC), power generation, and various industrial applications, including oil, gas, chemical, pharmaceutical, and food processing [4]. They are also crucial in enabling renewable energy technologies such as concentrating solar power (CSP) [5]. The specific energy (stored energy/mass) or energy transport density (transported energy rate/mass flow rate) of thermal fluids is given by $C\Delta T$, where C is the specific heat capacity of the fluid and ΔT is the temperature rise. The specific heat (C) of current thermal fluid technologies has remained significantly below that of water (4.2 J/g·K), which itself suffers from a relatively low boiling temperature (100 °C). Thermal fluid technologies capable of operating in extended temperature ranges require large quantities of fluid to compensate for low C, increasing pressure drop, cost and space requirements and requiring transport systems/pumps capable of large mass flow rate.

Conventional thermal fluids utilize noncovalent interactions such as hydrogen bonds (e.g., glycols), van der Waals forces (e.g., mineral oils), or electrostatic interactions (e.g., molten salts) to store heat, mechanisms that are arguably reaching their limits. One approach to increase the specific heat capacity involves the addition of micro-encapsulated phase change materials (PCM) to thermal fluids. For example, Yang *et al.* reported that the specific heat of the fluid polyalphaolefin (PAO) can increase by 56% (from 2.3 to 3.6 J/g·K) with 20 wt.% NPG-silica

microcapsules [6]. However, it requires the synthesis of micro-encapsulating materials, which greatly adds to the total cost of this technology. In addition, controlling the stability of the liquid suspensions poses further challenges for systems development.

In the early 1980s, the concept of using reversible liquid-phase chemical reactions to store heat for solar energy applications was proposed and tangentially explored [7, 8]. Using calorimetry, Sparks and Poling measured the heat of reaction and equilibrium constant for the Diels–Alder reaction between maleic anhydride and dilute 2-methylfuran [9]. They proposed that a hypothetical reaction mixture at a high concentration (7 mol/L) could achieve an apparent heat capacity of 7.37 J/cm^3·K, 76% higher than that of water. While the results seemed to be promising, the method for calculating this apparent heat capacity is neither explicit nor general. As a result, their work has been largely overlooked by the thermochemical energy storage community, and the concept of increasing specific heat of liquids by reversible chemical reactions has not been well developed.

Inspired by the pioneering work of Sparks and Poling [9], we formulated a simple mathematical model for the enhanced specific heat of liquids based on the temperature dependence of chemical equilibria in solution (liquid phase) and investigated the effects of various reaction parameters on the energy density and volumetric heat capacity of the liquids. We used density functional theory (DFT) calculations to accurately compute the reaction parameters such as the enthalpy and entropy of reaction at the molecular level. Combined with our macroscale model, molecular DFT calculations suggest that the energy density and specific heat of the material can be tuned through functionalization of the reacting molecules, thus providing a way to screen a large number of candidate reactions for subsequent experimental studies.

Macroscale Thermodynamic Model to Calculate Thermochemical Heat Capacity

Considering a generic exothermic reaction of the type $R_1 + R_2 = P$, the energy profile is shown in Figure 1. The two reactants (R_1 and R_2) overcome a kinetic barrier to form the product (P) as the reaction proceeds from the left to the right on the reaction coordinate. The amount of heat released is determined by the enthalpy of reaction, ΔH_{rxn}. If this reaction is reversible under suitable conditions, its reverse reaction represents an energy storage process (endothermic), where P absorbs heat to reform the original reactants (R_1 and R_2).

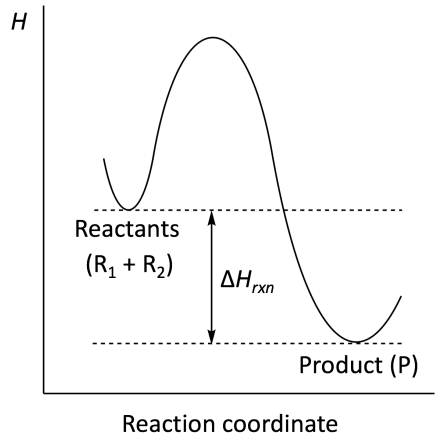

Figure 1. Reaction energy profile for a generic exothermic reaction $R_1 + R_2 = P$.

Our goal is to connect the fundamental chemical aspects of this reaction (e.g., ΔH_{rxn} and ΔS_{rxn}) that can be computed (using theoretical chemistry) or measured (using calorimetry or spectroscopy) to the effective volumetric heat capacity.

For a liquid phase reaction system that only consists of P initially (within a non-reacting solvent), and neither A nor B is present, we define a quantity c_{max}, to be the maximum molar concentration of P in mol/L. The initial concentrations of R_1, R_2 and P are 0, 0, and c_{max}, respectively (Figure 2).

At chemical equilibrium, the concentration of P is denoted by c ($0 < c < c_{max}$). The decrease in the concentration of P (i.e., $c_{max} - c$) is equal to the increase in the concentrations of R_1 and R_2, as a result of the reaction stoichiometry (one mole of P transforms into one mole of R_1 and one mole of R_2, assuming there is no change in volume). Thus, the corresponding concentrations of R_1 and R_2 are both $c_{max} - c$ at equilibrium.

	R_1 + R_2 ⇌	P
Initial concentration:	0 0	c_{max}
At equilibrium:	$c_{max} - c$ $c_{max} - c$	c

Figure 2. Illustration of the initial and equilibrium concentrations of R_1, R_2 and P.

The equilibrium constant K_{eq}, defined by the equilibrium concentrations of the reaction components, can thus be expressed by the equation

$$K_{eq} = \frac{c}{(c_{max} - c)^2}. \tag{1}$$

The van't Hoff equation [10] that relates the equilibrium constant, K_{eq}, to the temperature, T, is given by

$$\ln K_{eq}(T) = -\frac{\Delta H_{rxn}}{RT} + \frac{\Delta S_{rxn}}{R}, \tag{2}$$

where ΔH_{rxn} is the enthalpy of reaction, ΔS_{rxn} is the entropy of reaction and R is the universal gas constant.

For many reversible reactions, the equilibrium constants can be experimentally measured at different temperatures. The plot of ln K_{eq} versus $1/T$ (the van't Hoff plot) is widely used for experimentally determining the enthalpy and entropy of reaction. Eq. (2) can be rearranged to give

$$K_{eq}(T) = e^{\left(\frac{-\Delta H_{rxn}}{RT} + \frac{\Delta S_{rxn}}{R}\right)}, \tag{3}$$

and K_{eq} is expressed as a function of temperature T.

Solving for c in Eq. (1), we obtain

$$c(T) = \frac{\left(2c_{max} + \frac{1}{K_{eq}(T)}\right) - \sqrt{\left(2c_{max} + \frac{1}{K_{eq}(T)}\right)^2 - 4{c_{max}}^2}}{2}, \tag{4}$$

and the equilibrium concentration c is expressed as a function of temperature T.

A change in the concentration $c(T)$ with respect to a change in temperature corresponds to a partial reaction that converts a fraction of P into R_1 and R_2, or vice versa. The heat absorbed/released by such a partial reaction is always less than ΔH_{rxn}. In theory, only if the temperature changes from absolute zero to infinite high could P completely convert into R_1 and R_2 (when $T \rightarrow 0$K, $c(T) = c_{max}$, while when $T \rightarrow \infty$, $c(T) = 0$). Because enthalpy is a state function, the total enthalpy of the reaction mixture expressed as a function of temperature, $H(T)$, depends on a reference state at which the enthalpy is set to zero. For convenience, we define a low temperature T_{low} at which the equilibrium concentration of P is c_{low} and to which the enthalpy of the reaction mixture is referenced, *i.e.,* $H(T_{low}) = 0$. Because the conversion of P into R_1 and R_2 is a process that absorbs heat (endothermic), the equilibrium mixture mainly consists of P at a sufficiently low temperature, and an increase in temperature would shift the equilibrium towards R_1 and R_2 (Le Chatelier's principle). At any temperature T that is equal or greater than T_{low}, the enthalpy of the reaction mixture per unit volume (energy density) is given by

$$H(T) - H(T_{low}) = \Delta H_{rxn}\,(c(T) - c_{low}) + C_{p\_base}\,(T - T_{low}), \tag{5}$$

where C_{p_base} is the intrinsic volumetric heat capacity of the reaction mixture. The first term in Eq. (5) is the heat absorbed due to the net chemical reaction (shift of equilibrium) from T_{low} to T, and the second term is the sensible heat absorbed by the reaction mixture itself (R_1, R_2, P and solvent). For simplicity, we assume that C_{p_base} does not vary with temperature, thus can be treated as constant. It should be noted that in practice, the intrinsic C_p of the reaction mixture (C_{p_base}) will be temperature-dependent. This originates from the fact that the C_p of each component is temperature-dependent and the composition of the reaction mixture (determined by the concentration of each component) is also temperature-dependent. In general, the specific heat capacity of a pure liquid gradually increases with temperature, and its volume expands as well. As a result, the volumetric heat capacity could increase (e.g., ethanol) or decrease (e.g., water) with increased temperature.

The effective volumetric heat capacity of the reaction mixture, $C_p(T)$, could be expressed as the first derivative of $H(T)$ with respect to T, as

$$C_p(T) = \frac{dH(T)}{dT} = \Delta H_{rxn}\frac{dc}{dT} + C_{p\_base} = \Delta H_{rxn}\frac{dc}{dK_{eq}}\frac{dK_{eq}}{dT} + C_{p\_base}\,. \tag{6}$$

From Eq. (4), the derivative of c with respect to K_{eq} can be expressed as

$$\frac{dc}{dK_{eq}} = -\frac{1}{{K_{eq}}^2}\left(\frac{1}{2} - \frac{2c_{max} + \frac{1}{K_{eq}}}{2\sqrt{\left(2c_{max} + \frac{1}{K_{eq}}\right)^2 - 4{c_{max}}^2}}\right). \tag{7}$$

From Eq. (3), the derivative of K_{eq} with respect to T can be expressed as

$$\frac{dK_{eq}}{dT} = K_{eq}\frac{\Delta H_{rxn}}{RT^2}. \tag{8}$$

Substitute Eqs. (7) and (8) into (6), we obtain

$$C_p(T) = -\frac{(\Delta H_{rxn})^2}{RT^2 K_{eq}(T)}\left(\frac{1}{2} - \frac{2c_{max} + \frac{1}{K_{eq}(T)}}{2\sqrt{\left(2c_{max} + \frac{1}{K_{eq}(T)}\right)^2 - 4{c_{max}}^2}}\right) + C_{p\_base}. \tag{9}$$

Substitute Eq. (4) into Eq. (5), we obtain

$$H(T) - H(T_{low}) \tag{10}$$

$$= \Delta H_{rxn}\left(c_{max} - c_{low} + \frac{1}{2K_{eq}(T)} - \frac{1}{2}\sqrt{\left(2c_{max} + \frac{1}{K_{eq}(T)}\right)^2 - 4{c_{max}}^2}\right) + C_{p\_base}\,(T - T_{low}).$$

Combined with Eq. (3), Eqs. (9) and (10) are useful for plotting the enthalpy (energy density) and effective volumetric heat capacity of an equilibrium reaction mixture versus temperature. To test the utility of our model, we apply it to the Diels–Alder (DA) reaction between 2-methylfuran and maleic anhydride (Figure 3), which has been suggested by Sparks and Poling as potentially useful for thermal storage [9].

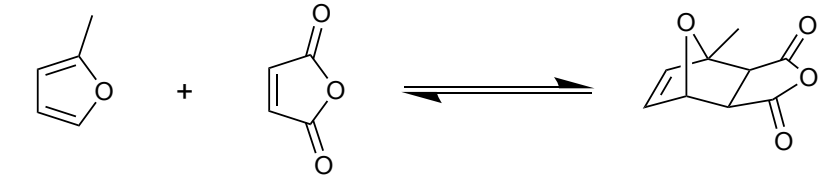

2-methylfuran maleic anhydride *exo*-DA-product

Figure 3. Thermally reversible Diels–Alder reaction between 2-methylfuran and maleic anhydride.

The enthalpy of reaction (ΔH_{rxn}) has been determined to be -14.3 kcal/mol by calorimetry [9]. The equilibrium constant (K_{eq}) was measured to be 0.614 L/mol at 45 °C, from which the entropy of reaction (ΔS_{rxn}) can be calculated (-45.9 cal/mol·K) using Eq. (2). For simplicity, we assume an intrinsic volumetric heat capacity of 2.0 J/cm^3·K for reactions carried out in an organic solvent. The mass density, specific heat and volumetric heat capacity of some common organic solvents are summarized and shown in Supplementary Table 1, supporting that this is a reasonable approximation. The energy density (increase in enthalpy from T_{low} to T) and the effective volumetric heat capacity of the above reaction versus temperature according to our derivation are plotted in Figure 4, with a maximum concentration of the product (c_{max}) set to 1.0 mol/L (standard condition). It should be noted that in real applications, the maximum concentration will be limited by solubility.

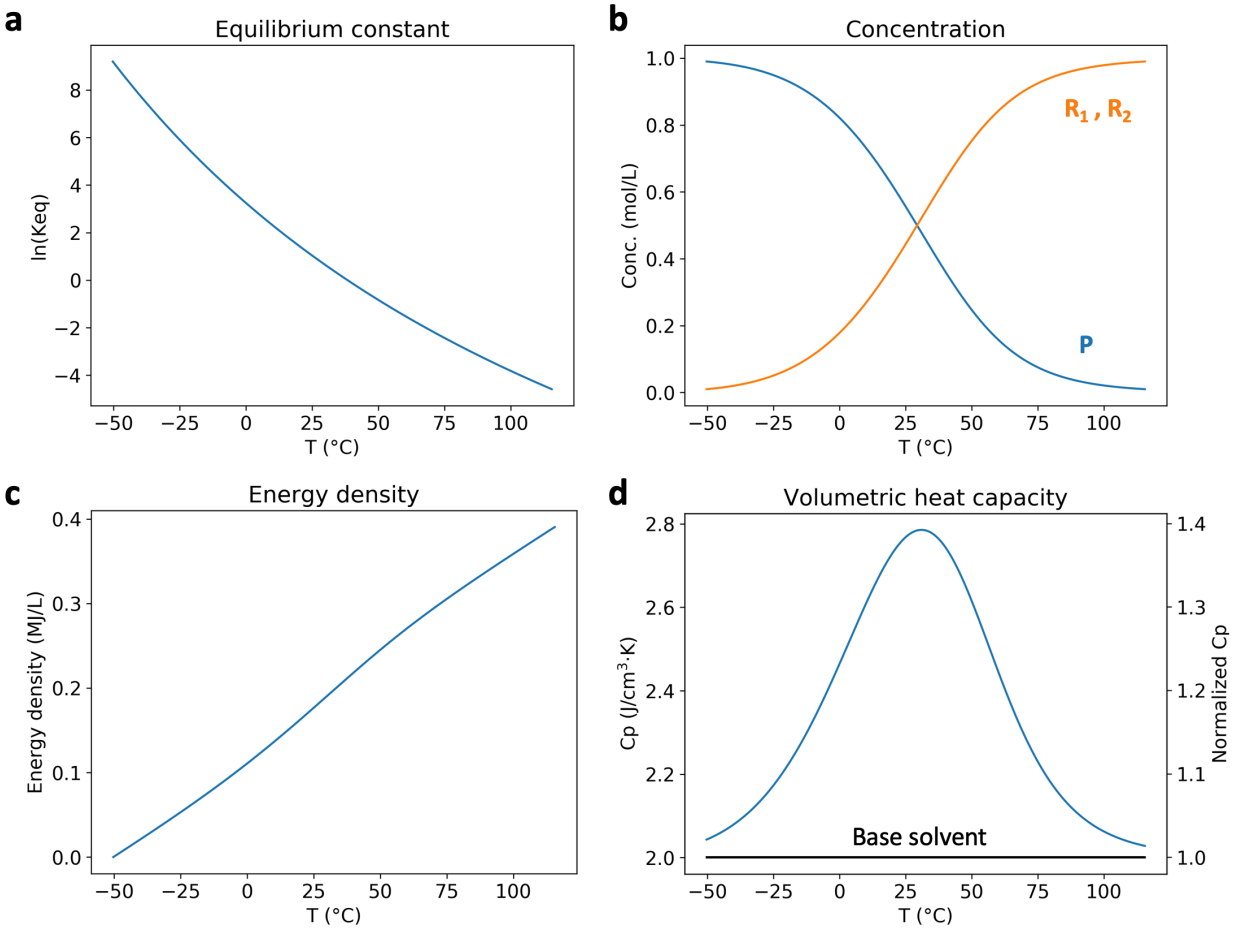

Figure 4. Plots of the equilibrium constant, concentration, enthalpy (energy density) and the effective volumetric heat capacity versus temperature, for the reversible Diels–Alder reaction between 2-methylfuran and maleic anhydride, with a maximum concentration of 1.0 mol/L.

For the plots shown in Figure 4, the low temperature limit T_{low} is defined at which $c = 0.99c_{max}$ (i.e., $c_i = 0.99c_{max}$ and the reaction mixture mainly consists of P), thus, the corresponding high temperature limit (T_{high}) is chosen as the temperature at which $c = 0.01c_{max}$ (the reaction mixture mainly consists of R_1 and R_2). T_{low} and T_{high} can be obtained from Eqs. (1) and (2). In practice, the actual temperature range should be within the melting and boiling temperatures of the liquids. For a solution with the maximum concentration of the product being 1.0 mol/L, the highest heat

capacity is 2.8 J/cm^3·K at 26 °C (room temperature). The relative increase (40%) in effective heat capacity depends on the heat capacity of the solvent or the reaction mixture (C_{p_base}), while the absolute increase (0.8 J/cm^3·K) does not. This absolute increase solely depends on the reaction parameters. For higher energy density and heat capacity, a higher concentration would be needed, which is limited by the solubility of the corresponding reactants/product. It has been suggested [9] that a concentration of 7.0 mol/L could be potentially reached for the reaction shown in Figure 3. Therefore, we also plotted the energy density and volumetric heat capacity with c_{max} set to 7.0 mol/L. The results are shown in Figure 5. The intrinsic heat capacity (base) is taken from ref. [9] as 2.638 J/cm^3·K.

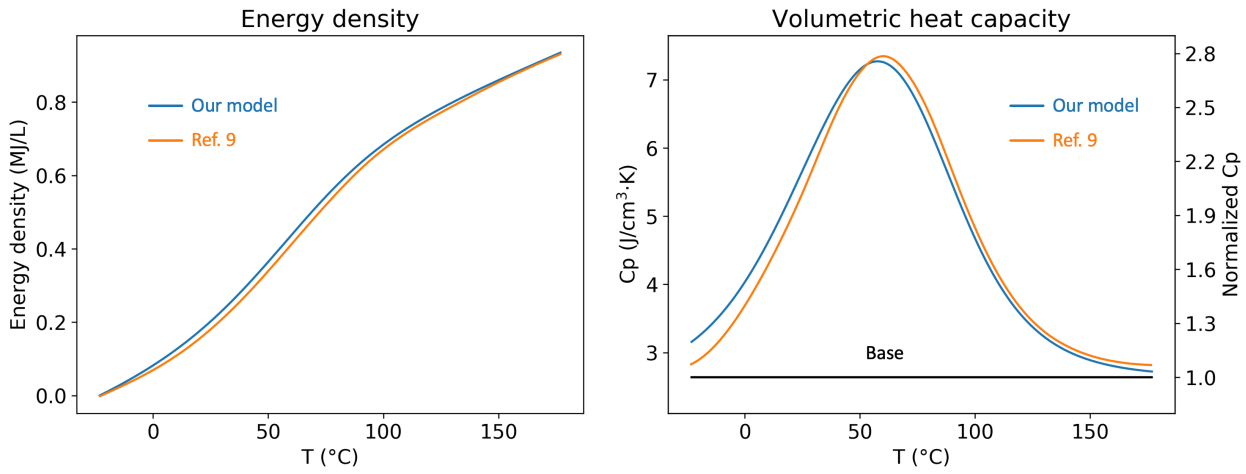

Figure 5. Plots of volumetric energy density and the volumetric heat capacity versus temperature, for the reversible Diels–Alder reaction between 2-methylfuran and maleic anhydride, with a maximum concentration of 7.0 mol/L.

The blue curves shown in Figure 5 are very close to the curves (orange) for H and C_p by Sparks and Poling (extracted using a graph digitizer), but without the need of experimentally measured C_p values for all the reaction components and presumably numerical integrals to calculate the

enthalpy of the mixtures. Therefore, our simple and general model with only analytical expressions of H and C_p is very useful in exploring the effects of various reaction parameters (c_{max}, ΔH_{rxn}, and ΔS_{rxn}). The results in Figures 4 and 5 already demonstrate that the concentration has a large influence on the energy density and volumetric heat capacity. We next explore these effects by varying one parameter and keeping the other two parameters constant, and the results are shown in Figure 6. A base line for the pure solvent that has a C_p of 2.0 J/cm^3·K is also shown for comparison.

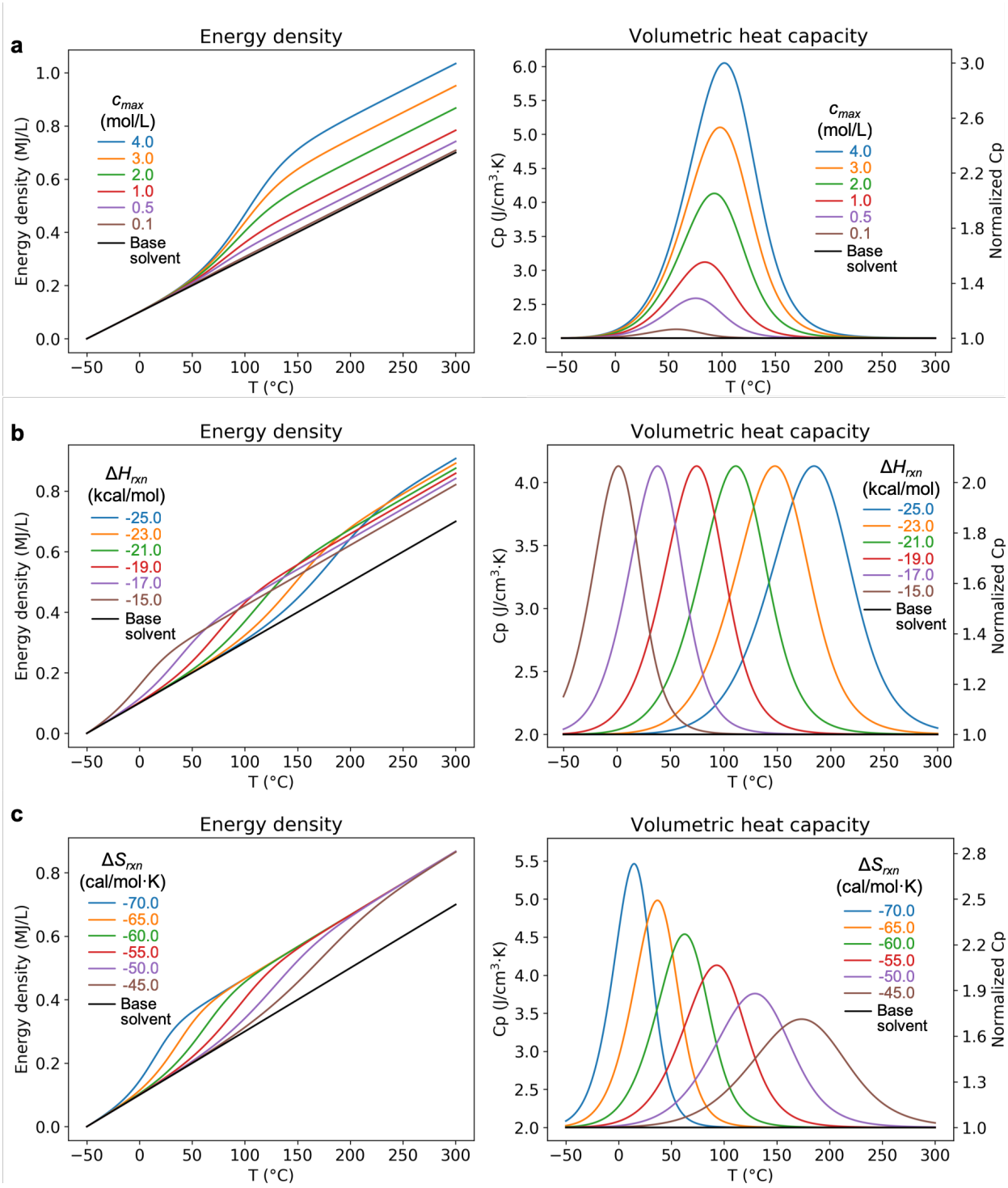

Figure 6. Effects of different reaction parameters on the energy density and the volumetric heat capacity of a thermochemical energy storage system. **a**, Modeled concentration effect with c_{max} varied from 0.1 to 4.0 mol/L, ΔH_{rxn} = -20.0 kcal/mol and ΔS_{rxn} = -55.0 cal/mol·K. **b**, Modeled

enthalpy effect with ΔH_{rxn} varied from -15.0 to -25.0 kcal/mol, ΔS_{rxn} = -55.0 cal/mol·K and c_{max} = 2.0 mol/L. **c**, Modeled entropy effect with ΔS_{rxn} varied from -45.0 to -70.0 cal/mol·K, ΔH_{rxn} = -20.0 kcal/mol and c_{max} = 2.0 mol/L.

The results of the modeling in Figure 6a show that dissolving moderate to high concentrations of reactants/product into a base solvent with moderate heat capacity (2.0 J/cm^3·K) can enhance the maximum heat capacity of the resulting solution beyond even that of liquid water (4.2 J/cm^3·K). In practice, the achievable concentration would be limited by the solubility of the reactants/product in the base solvent. Furthermore, by tuning ΔH_{rxn}, one can control the temperature range in which the enhancement is attained (Figure 6b). Counter-intuitively, the value of ΔH_{rxn} does not affect the maximum C_p attained. Instead, it affects the area under curve (AUC) of C_p, which is related to the energy storage capacity of the liquid mixture. The more negative ΔH_{rxn}, the more thermal energy can be stored by the liquid mixture. By further tuning the ΔS_{rxn}, one can also control the width of the enhancement region of C_p (e.g., sharply peaked or broadened across a wide range), as measured by the full width at half maximum (FWHM). In addition, with more negative ΔS_{rxn}, the maximum C_p is larger, and the corresponding temperature at $C_{p,\,max}$ is lower. These results indicate that by tuning the fundamental properties (ΔH_{rxn} and ΔS_{rxn}) of the underlying reaction and the amount of dissolved species (c_{max}), one can produce a spectrum of technologies tailored to specific applications at different temperatures. Table 1 summarizes the qualitative effects of adjusting these parameters on the thermodynamic properties relevant for thermal storage applications.

Table 1. Qualitative effects of reaction parameters on the thermodynamic properties of the reaction mixture.

	T at $C_{p,\,max}$	$C_{p,\,max}$	$C_{p,\,FWHM}$	Energy density

c_{max} ↑	↑	↑	↑	↑
$\lvert\Delta H_{rxn}\rvert$ ↑	↑	—	↑	↑
$\lvert\Delta S_{rxn}\rvert$ ↑	↓	↑	↓	—

Molecular Models to Calculate ΔH_{rxn} and ΔS_{rxn}

With these results from our macroscale equilibrium thermodynamics model, we next explored the effects of tuning molecular structures on the thermodynamic parameters of the reaction. For practical considerations, the 2-methylfuran/maleic anhydride Diels–Alder reaction shown in Figure 3 would not be applicable for higher temperature thermal storage, due to the relatively low boiling point of 2-methylfuran (63 °C). To increase the boiling points, we increased the sizes of the reactants and the corresponding product, by adding larger substituents (fused benzene, phenyl group, and methyl group) on these molecules (Figure 7). It has been shown that substitution could tune the energetics in similar Diels–Alder reactions [11]. The boiling points of the modified reactants in Figure 7 are 437.5 and 223 °C, respectively [12]. Their product, which has higher molecular weight, is predicted to have a higher boiling point. In general, boiling is a very important consideration in choosing a fluid for thermal storage. The boiling point of known compounds could be extracted from a variety of online databases, such as the ChemSpider database [12], the CRC Handbook of Chemistry and Physics [13], and the NIST Chemistry WebBook [14], etc. For compounds without experimental boiling point data, ChemSpider [12] provides various quantitative structure–property relationships (QSPR) models that can be used to predict the boiling point.

We then performed density functional theory (DFT) calculations to obtain the reaction enthalpy and entropy values for the modified reaction shown in Figure 7. DFT calculations were performed

using the Q-Chem code [15]. Structural optimizations and vibrational frequency calculations were carried out with the ωB97X-D functional [16] with the 6-31G(d) basis set. Subsequent single-point energy calculations using a larger 6-311++G(d,p) basis set were performed to obtain more accurate reaction energies (see Supplementary File for computational details). DFT calculations, which provide relatively accurate energetics with reasonable computational cost, have been widely used to study reaction mechanisms and selectivities of organic reactions including the Diels–Alder reaction [17–19]. The computed reaction enthalpy and entropy for the 2-methylfuran/maleic anhydride reaction agree well the experimentally measured values (Figure 7, expt. ΔH_{rxn} = -14.3 kcal/mol, comp. ΔH_{rxn} = -14.5 kcal/mol; expt. ΔS_{rxn} = -45.9 cal/mol·K, comp. ΔS_{rxn} = -44.6 cal/mol·K). However, it is worth noting that the accurate computation of absolute entropies in solution is more challenging compared to that in the gas phase, as a result of potentially close interactions between solute and solvent molecules [20, 21]. In the case of calculating reaction entropies, this problem is to some extent alleviated due to the nature of the thermodynamic quantities that are of interest, namely the changes in entropy during the reaction (relative entropies). Assuming the interactions between the product and the reactants are similar to those between the reactants and the solvent, thermodynamic properties computed in the gas phase can reproduce experimental results, as exemplified by the results shown in Figure 7. We note that we have also compared the gas phase values to the those computed using the polarizable continuum model (PCM) [22], which is an implicit solvent method that considers some aspects (i.e., the dielectric effects) of solution thermochemistry. The results are qualitatively the same, as expected. In some cases, however, the above assumptions may not hold, especially when solutes interact strongly or react with the solvent [23, 24]. More sophisticated quantum mechanical calculations using explicit solvent cluster models in which the solvent configurations are properly sampled may

be needed in such cases, but the cost for computational screening would be prohibitively high. Such techniques could in principle be explored for the most promising reactions from a computational study, or to better understand unexpected experimental results.

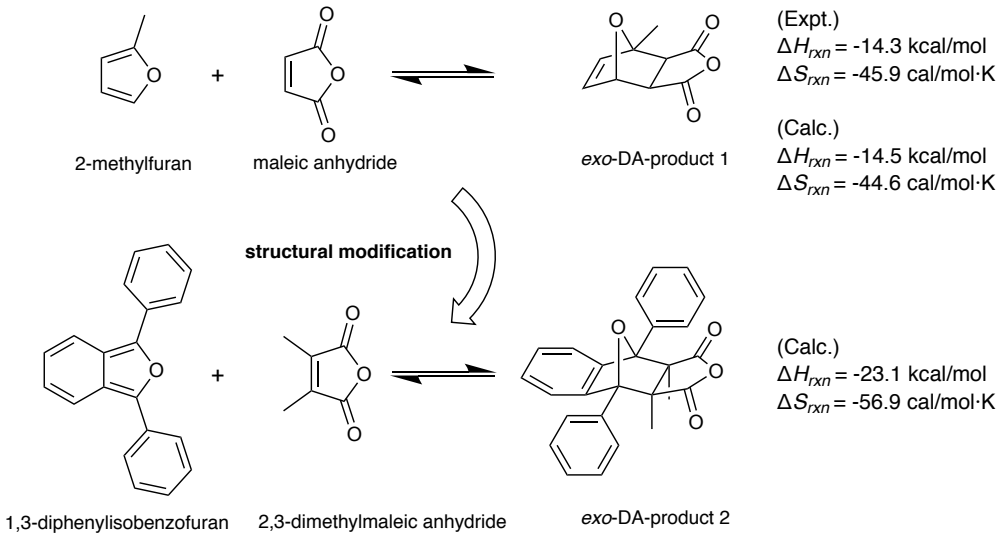

Figure 7. Structural modification of the 2-methylfuran/maleic anhydride Diels–Alder reaction.

It was found that these structural modifications could change the fundamental reaction parameters (ΔH_{rxn} and ΔS_{rxn}). Specifically, the formation of an aromatic ring structure (fused benzene ring) results in an increased energy release for the new reaction, as the ΔH_{rxn} is -21.6 kcal/mol compared to -14.3 kcal/mol in the original reaction. The ΔS_{rxn} becomes more negative (from -45.9 to -59.2 cal/mol·K) as well, likely due to the larger decrease in the degree of freedom of the resulting structure (more sterically congested and more rigid). The results from the DFT calculations provide some guiding principles for designing new reaction systems that have desired thermodynamic parameters to be used for thermal storage at different temperatures. For example, adding substituents at the reaction sites leads to a more negative ΔS_{rxn}. However, this trend needs to be further validated by a more comprehensive study of a series of reactions.

We next plotted the predicted energy density and volumetric heat capacity of this new reaction using our theoretical model. The results are summarized in Figure 8. For comparison, the corresponding curves for water and a commercially available thermal fluid (Dowtherm A) are also shown. The predicted properties of this new reaction (blue curves) has the potential to reach an energy density of 0.72 MJ/L in the temperature range of 15–255 °C, representing a 50% increase in the stored energy as compared to the base solvent (0.48 MJ/L).

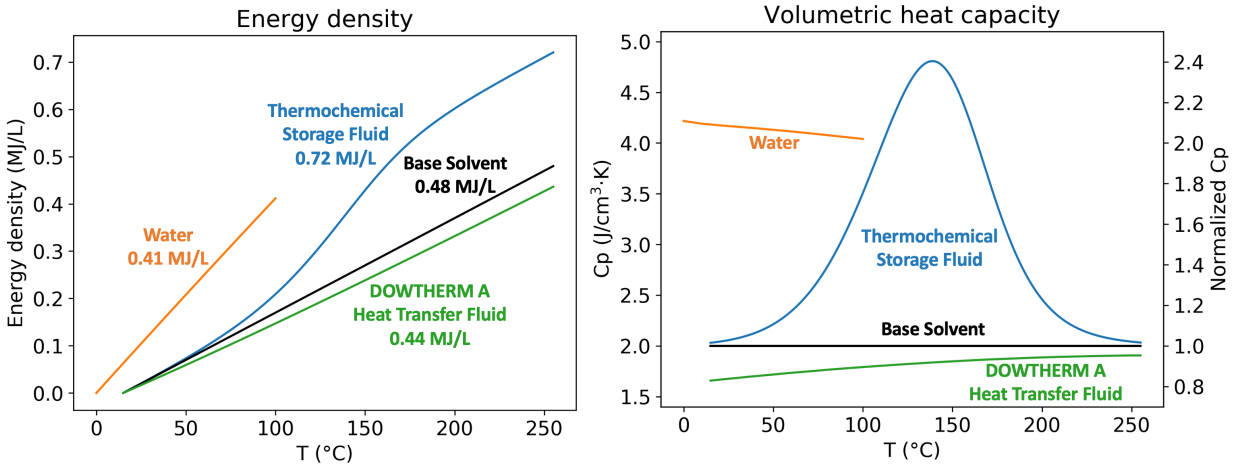

Figure 8. Plots of the enthalpy (energy density) and the volumetric heat capacity versus temperature, for the reversible Diels–Alder reaction between 1,3-diphenylisobenzofuran and 2,3-dimethylmaleic anhydride, with a maximum concentration of 2.5 mol/L. Data for water [25,26] and a typical heat transfer fluid (Dowtherm A [27]) are also presented.

An interesting comparison between thermochemical fluids with fluids based on both sensible and latent heat such as PCMs would be best contrasted with a comparison between the enthalpy of reaction (ΔH_{rxn}) to the enthalpy of fusion (ΔH_{fus}), as both types of fluids have the contribution from sensible heat. For example, thermochemical fluids with ΔH_{rxn} ranging from -15.0 to -25.0 kcal/mol (as data shown in Figure 6b), a concentration of 2.0 mol/L and a mass density of 1kg/L have ΔH_{rxn}

of 125 to 209 kJ/kg, which are comparable to a common type of phase change material–salt hydrates, with ΔH_{fus} ranging from 125 to 280 kJ/kg (data for eight representative salt hydrates reviewed by Pereira da Cunha and Eames [28]). While reaction kinetics may be a potential problem for thermochemical fluids, just as supercooling for PCMs, thermochemical fluids do not have the problem of phase separation or the need for micro-encapsulation.

One major limitation of our model is the assumption of equilibrium conditions at various temperatures. For practical applications, the reaction kinetics will be important as it may take time for the reaction mixtures to reach equilibrium, especially at lower temperatures. One simplification in our model is that C_{p_base} is assumed as temperature-independent. Using the average intrinsic C_p over a temperature range as the baseline greatly simplify our analysis, without affecting the total energy density. However, it should be noted that the temperature-dependent nature of C_{p_base} will affect the actual C_p curve of a specific thermochemical fluid in practice. For our theoretical model, since the effective heat capacity consists of two parts that are additive (the heat capacity due to the reaction and C_{p_base}), the temperature-dependent nature of C_{p_base} will in principle not affect the qualitative trends presented in Figure 6, in which the main differences between the curves originate from the reaction parameters. However, we note that it is relatively easy to add a temperature dependent intrinsic heat capacity to the theoretical analysis as long as temperature dependent behavior is known. Another potential risk of developing a thermal storage liquid based on chemical reactions is the reversibility (cyclability) of such reactions. Potential side reactions need to be dealt with and overcome for any real applications of such technologies. In addition, viscosity of the fluid is an important parameter in determining the pumping power, and will ultimately influence the performance of such a thermochemical fluid. In principle, adding reactive components will not dramatically change the viscosity of the base fluids, unless these species interact strongly with the

solvent molecules, for example, through strong ionic or hydrogen bonds. In practice, the viscosity of the thermochemical fluid needs to be experimentally measured, but the intrinsic viscosity of the base fluid would serve as a reasonable indicator in the early stage of reaction design. For example, the viscosity of a common organic solvent–DMF (*N*,*N*-dimethyl formamide) is 0.92 cP at 20 °C, which is similar to that of water (1.00 cP). A DMF-based Diels–Alder mixture of 2-methylfuran/maleic anhydride is likely to have its viscosity being close to this value. Extensive experimental studies need to be performed to finally select the best reactions for thermochemical storage in the liquid phase. Nevertheless, our macroscale thermodynamic model provides a simple and direct approach to evaluate reactions for such applications, especially when combined with high-throughput computational screening tools (such as molecular DFT calculations) [29, 30] . These will enable us to search for the most promising candidate reactions for further experimental studies.

Conclusions

In summary, we have developed a macroscale thermodynamic model that connects fundamental properties of a thermally reversible chemical reaction to the thermophysical properties of a liquid that consists of such a reaction mixture, based on the classical theory of equilibrium thermodynamics. This framework allows us to employ a state-of-the-art computational screening method such as DFT calculations to identify suitable molecular systems for thermochemical energy storage applications. Modeling and preliminary DFT results demonstrate the tunability of energy density and heat capacity enhancement with a reversible Diels–Alder reaction. These findings open up new avenues for thermal energy storage that can break traditional barriers to achieve high specific heat and energy storage capacity. With this, we aim to develop a few

transportable, high thermal energy density liquids that can be potentially employed for grid storage, building thermal management, or enhanced thermal energy recovery in industrial applications.

Acknowledgement

This research was supported by the Laboratory Directed Research and Development Program (LDRD) at Lawrence Berkeley National Laboratory under Contract No. DE-AC02-05CH11231. This research used resources of the National Energy Research Scientific Computing Center (NERSC), a U.S. Department of Energy Office of Science User Facility operated under Contract No. DE-AC02-05CH11231.

References

[1] H. Zhang, J. Baeyens, G. Cáceres, J. Degrève, and Y. Lv, "Thermal energy storage: Recent developments and practical aspects," *Prog. Energy Combust. Sci.*, vol. 53, pp. 1–40, 2015.

[2] D. Aydin, S. P. Casey, and S. Riffat, "The latest advancements on thermochemical heat storage systems," *Renew. Sustain. Energy Rev.*, vol. 41, pp. 356–367, 2015.

[3] I. Gur, K. Sawyer, and R. Prasher, "Searching for a better thermal battery," *Science*, vol. 335, no. 6075, pp. 1454–1455, 2012.

[4] H. Inaba, "New challenge in advanced thermal energy transportation using functionally thermal fluids," *Int. J. Therm. Sci.*, vol. 39, no. 9–11, pp. 991–1003, Oct. 2000.

[5] S. Kuravi, J. Trahan, D. Y. Goswami, M. M. Rahman, and E. K. Stefanakos, "Thermal energy storage technologies and systems for concentrating solar power plants," *Prog. Energy Combust. Sci.*, vol. 39, no. 4, pp. 285–319, 2013.

[6] F. Cao, J. Ye, and B. Yang, "Synthesis and characterization of solid-state phase change material microcapsules for thermal management applications," *J. Nanotechnol. Eng. Med.*, vol. 4, no. 4, p. 041001, Mar. 2014.

[7] M. L. Mastroianni and B. E. Poling, "Energy storage capacities of reversible liquid phase chemical reactions," *Thermochim. Acta*, vol. 53, no. 2, pp. 141–147, Feb. 1982.

[8] T. G. Lenz, L. S. Hegedus, and J. D. Vaughan, "Liquid phase thermochemical energy conversion systems—An application of Diels-Alder chemistry," *Int. J. Energy Res.*, vol. 6, no. 4, pp. 357–365, Jan. 1982.

[9] B. G. Sparks and B. E. Poling, "Energy storage capacity of reversible liquid-phase Diels Alder reaction between maleic anhydride and 2-methyl furan," *AIChE J.*, vol. 29, no. 4, pp. 534–537, Jul. 1983.

[10] P. Atkins and J. De Paula, *Physical Chemistry*, 8th ed. W. H. Freeman and Company, 2006.

[11] Z. Shi *et al.*, "Tuning the Kinetics and Energetics of Diels–Alder Cycloaddition Reactions to Improve Poling Efficiency and Thermal Stability of High-Temperature Cross-Linked Electro-Optic Polymers," *Chem. Mater.*, vol. 22, no. 19, pp. 5601–5608, Oct. 2010.

[12] The Royal Society Of Chemistry, "ChemSpider," *The Royal Society Of Chemistry*. [Online]. Available: http://www.chemspider.com. [Accessed: 14-Mar-2019].

[13] J. R. Rumble, "CRC Handbook of Chemistry and Physics, 99th Edition, 2018-2019," *Handbook of Chemistry and Physics*. [Online]. Available: http://www.hbcponline.com/. [Accessed: 14-Mar-2019].

[14] P. J. Linstrom and W. G. Mallard, *NIST Chemistry webBook, NIST Standard Reference Database Number 69*. 2014.

[15] Y. Shao *et al.*, "Advances in molecular quantum chemistry contained in the Q-Chem 4 program package," *Mol. Phys.*, vol. 113, no. 2, pp. 184–215, 2015.

[16] J. Da Chai and M. Head-Gordon, "Long-range corrected hybrid density functionals with damped atom-atom dispersion corrections," *Phys. Chem. Chem. Phys.*, vol. 10, pp. 6615–6620, 2008.

[17] E. Goldstein, B. Beno, and K. N. Houk, "Density functional theory prediction of the relative energies and isotope effects for the concerted and stepwise mechanisms of the Diels-Alder reaction of butadiene and ethylene," *J. Am. Chem. Soc.*, vol. 118, no. 25, pp. 6036–6043, 1996.

[18] J. S. Barber *et al.*, "Diels–Alder cycloadditions of strained azacyclic allenes," *Nat. Chem.*, vol. 10, pp. 953–960, 2018.

[19] P. Yu, W. Li, and K. N. Houk, "Mechanisms and origins of selectivities of the Lewis acid-catalyzed Diels–Alder reactions between arylallenes and acrylates," *J. Org. Chem.*, vol. 82, no. 12, pp. 6398–6402, 2017.

[20] J. P. Guthrie, "Use of DFT methods for the calculation of the entropy of gas phase organic molecules: An examination of the quality of results from a simple approach," *J. Phys. Chem. A*, vol. 105, no. 37, pp. 8495–8499, 2001.

[21] Y. Li and D. C. Fang, "DFT calculations on kinetic data for some [4+2] reactions in solution," *Phys. Chem. Chem. Phys.*, vol. 16, no. 29, pp. 15224–15230, 2014.

[22] B. Mennucci *et al*., "Polarizable continuum model (PCM) calculations of solvent effects on optical rotations of chiral molecules," *J. Phys. Chem. A*, vol. 106, no. 25, pp. 6102–6113, 2002.

[23] Y. F. Yang, P. Yu, and K. N. Houk, "Computational Exploration of Concerted and Zwitterionic Mechanisms of Diels-Alder Reactions between 1,2,3-Triazines and Enamines and Acceleration by Hydrogen-Bonding Solvents," *J. Am. Chem. Soc*., vol. 139, no. 50, pp. 18213–18221, 2017.

[24] Z. Yang *et al*., "Influence of water and enzyme SpnF on the dynamics and energetics of the ambimodal [6+4]/[4+2] cycloaddition," *Proc. Natl. Acad. Sci. U. S. A*., vol. 115, no. 5, pp. E848–E855, 2018.

[25] The Engineering ToolBox, "Water - Heat Capacity (Specific Heat)," *The Engineering ToolBox.com*, 2004. [Online]. Available: https://www.engineeringtoolbox.com/specific-heat-capacity-water-d_660.html.

[26] The Engineering Toolbox, "Water - Density, Specific Weight and Thermal Expansion Coefficient," *www.engineeringtoolbox.com*, 2003. [Online]. Available: https://www.engineeringtoolbox.com/water-density-specific-weight-d_595.html. [Accessed: 14-Mar-2019].

[27] "DOWTHERM A Heat Transfer Fluid, Product Technical Data." [Online]. Available: http://msdssearch.dow.com/PublishedLiteratureDOWCOM/dh_0030/0901b803800303cd.pdf. [Accessed: 14-Mar-2019].

[28] J. Pereira da Cunha and P. Eames, "Thermal energy storage for low and medium temperature applications using phase change materials – A review," *Appl. Energy*, vol. 177, pp. 227–238, Sep. 2016.

[29] X. Qu *et al*., "The Electrolyte Genome project: A big data approach in battery materials discovery," *Comput. Mater. Sci*., vol. 103, pp. 56–67, 2015.

[30] L. Cheng *et al*., "Accelerating electrolyte discovery for energy storage with high-throughput screening," *J. Phys. Chem. Lett*., vol. 6, no. 2, pp. 283–291, Jan. 2015.